RSC Advances

ROYAL SOCIETY
OF CHEMISTRY

www.rsc.org/advances

Graphical Abstract
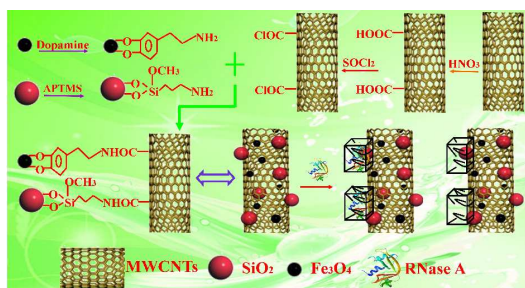
A new functional material Fe_3O_4/MWCNTs/SiO_2 was served as supporting material to

prepare SMIP for CL determination of RNase A

1   **Biorecognition and highly sensitive determination of Ribonuclease A**

2   **with chemiluminescence sensor based on Fe_3O_4/multi-walled carbon**

3   **nanotubes/SiO_2-surface molecular imprinting polymer**

4   Huimin Duan, Leilei Li, Xiaojiao Wang, Yanhui Wang, Jianbo Li, Chuannan Luo*

5   Key Laboratory of Chemical Sensing & Analysis in Universities of Shandong (University of

6   Jinan), School of Chemistry and Chemical Engineering, University of Jinan, Jinan 250022, China

7   * Corresponding author. Tel.: +86 0531 89736065. E-mail address: chm_luocn@ujn.edu.cn.

8   **Abstract**

9   Here, a chemiluminescence (CL) sensor with high sensitivity and selectivity has

10   been developed for the determination of Ribonuclease A (RNase A). A new material

11   Fe_3O_4/multi-walled carbon nanotubes/SiO_2 (Fe_3O_4/MWCNTs/SiO_2) was introduced

12   into this sensor as supporting material to prepare surface molecular imprinting

13   polymer (SMIP). In this work, Fe_3O_4 could not only serve as backbone material in the

14   preparation of RNase A SMIP, but also as separation reagent to make the collection of

15   SMIP complex easily, carbon nanotube and SiO_2 was used as supporting material to

16   bear SMIP for their large specific surface area. Then, the nanocomposite of

17   Fe_3O_4/MWCNTs/SiO_2 was characterized by scanning electron microscopy (SEM),

18   X-ray diffraction (XRD) and Fourier transform infrared spectroscopy (FT-IR)

19   techniques. The adsorption ability of Fe_3O_4/MWCNTs/SiO_2-SMIP was calculated to

20   be 102 mg/g and it demonstrated the excellent recognition and adsorption ability of

21   the imprinting cavities situated at or in the proximity of the surface of the

22   Fe_3O_4/MWCNTs/SiO_2. Under the optimal conditions, the linear range extended from

23   1.0×10^{-9} mg/mL to 1.0×10^{-7} mg/mL for RNase A and the detection limit was 3.2 $\times$

24   10^{-10} mg/mL (3δ). The proposed sensor was successfully applied in determination of

25   RNase A in biological samples with recoveries from 93% to 105%.

26   **Keyword:** Ribonuclease A; chemiluminescence; Fe_3O_4/multi-walled carbon

27   nanotubes/SiO_2; surface molecular imprinting polymer; biorecognition

28   **1. Introduction**

29   As an endoribonuclease which could cut the 3 'end of RNA pyrimidine residues

30   specificly [1], Ribonuclease A (RNase A) has played a crucial role as a model system

31   in the studies of protein structure, enzymology, chemistry of proteins and enzyme

32   catalysis in the past decades [2]. The antitumor effect of RNase A shortly after its

33   isolation was investigated by Ledoux and it was very inspiring in the work of

34   anti-ascites tumors [3]. Over the last and present century, the research of RNase A

35   was focus on the analysis of RNA sequence and nucleic acids structure, the

36   protection and detection of RNase, the function of RNase A in the purification of

37   DNA and the diagnosis and treatment of Hepatitis B and tumor disease [4]. The

38   detection of RNase A was highly useful in diagnostic medicine as its level in the

39   blood serum could be a diagnostic marker for many diseases, including Myocardial

40   Infarction and Pancreatic Cancer [5, 6].

41   Molecular imprinting polymers (MIP) possessed high selective recognition and

42   capture capabilities. In 1949, F.H. Dickey [7] pioneered the concept of "specificity

43   adsorption" which was regarded as the seed of molecular imprinting technology. In

44   1973, Wulff and his co-workers synthesized MIP for the first time, which could

45   contribute to higher accuracy and lower detection limit for the template-monomer

46   complex (targer molecule) [8, 9]. Then, the development of molecular imprinting

47   technique was shown to the world. Afterwards, surface molecular imprinting

48 technique was proposed. By attaching the biomolecule to or close to the surface of the

49 polymer [10, 11], the mass transfer was improved and the removal rate of biomolecule

50 was promoted for the imprinting sites enabling easy access to the target protein

51 molecules [12]. While expediting the pace of the polymerization in significant

52 measure, atom transfer radical polymerization was firstly introduced into the

53 preparation of myoglobin surface molecular imprinting polymer (SMIP) by grafting

54 on silicon surface [13], which could be initiated in moderate temperature and even in

55 the presence of a small amount of oxygen.

56   Fe_3O_4 nanoparticles could be easily separated from complex matrix samples with

57 an external magnetic field, and was superior to centrifugation which needed

58 complicated steps and wasted a lot of time and energy. Due to its easy preparation,

59 good biocompatibility and environment benign, Fe_3O_4 nanoparticles were the

60 potential materials and have been widely applied in many fields such as sorbent [14],

61 sensor [15] and probe [16] et al. Gai and his co-workers prepared super paramagnetic

62 lysozyme SMIP by grafting the imprinting polymer on magnetic particles in aqueous

63 media, and researched its application in protein separation [17]. Dopamine could be

64 used as a robust anchor to immobilize functional molecules on the surface of Fe_3O_4

65 nanoparticles according to Xu′s work in 2004, which promised broad potential

66 applications of Fe_3O_4 nanoparticles [18] due to the excellent properties of inherent

67 biocompatibility, hydrophilicity and chemical stability. Dopamine could prevent the

68 aggregation of Fe_3O_4 nanoparticles and reduce the toxicity and oxidation of the Fe_3O_4

69 nanoparticles. Meanwhile, dopamine possessed abundant hydroxyl and amino groups

70 which could be used for further modification or react with varieties of substance [19,

71 20]. In recent years, SiO_2 nanoparticles have drawn considerable attention because of

72 the fundamental scientific interest [21]. With the advantages of good chemical

3

73   stability, large specific surface area and excellent biocompatibility, SiO_2 nanoparticles

74   were used to prepared lysozyme SMIP for noncovalent template sorption [22].

75   Multi-walled carbon nanotubes (MWCNTs) were a kind of typical one-dimensional

76   nanomaterials which possessed significant properties, such as high specific surface

77   area, good chemical stability, low toxicity and biocompatibility. Zhang et al. discussed

78   the preparation and characteristics of bovine serum albumin imprinting layers on the

79   surface of MWCNTs [23]. During the past decades, increasing interest has been paid

80   on MWCNTs as new sensing materials [24].

81   In the present study, with the merits of Fe_3O_4, SiO_2 and MWCNTs, a new

82   material-Fe_3O_4/MWCNTs/SiO_2 was synthesized and served as scaffold material to

83   prepare RNase A SMIP. In general, Fe_3O_4 was not only served as backbone material

84   to prepare RNase A SMIP, but also as separation material to separate SMIP complex,

85   carbon nanotube and SiO_2 was used as supporting material to bear SMIP for their

86   large specific surface area. Compared with core-shell $Fe_3O_4@SiO_2$/MWCNTs

87   nanocomposite [25], Fe_3O_4 could not only serve as backbone material in the

88   preparation of RNase A SMIP, but also as separation reagent to make the segregator

89   to separate collection of SMIP complex easily. The Fe_3O_4/MWCNTs/SiO_2-SMIP

90   exhibited excellent recognition and adsorption ability to RNase A owing to the

91   imprinting cavities situated at or in the proximity of the material's surface. Then, a

92   sensitive and selective chemiluminescence (CL) sensor for determination of RNase A

93   was proposed based on Fe_3O_4/MWCNTs/SiO_2-SMIP. At the optimal conditions of CL,

94   the proposed sensor was successfully applied in determination of RNase A in real

95   samples with high accuracy, sensitivity and selectivity.

2 Experiment

2.1 Chemicals and materials

RNase A, Thionyl chloride (A.R), Tetraethyl silicate (TEOS, A.R), Ferrous sulfate(A.R), Dimethyl formamide (DMF, 99%), Acrylamide (AM, 99%), Methacrylic acid (MAA), Ethylene glycol dimethyl acrylate (EGDMA, A.R), and Ammonium persulphate (APS, AR) were supplied by Sinopharm Chemical Reagent Co. Ltd (China); Anhydrous tetrahydrofuran (99%), N-N methylene double acrylamide (EP, A.R), N,N,N',N'-tetramethyl ethylenediamine (TEMED, A.R), 3-aminopropyltrimethoxysilane (APTMS, 97%) and Diethyl amino ethyl methacrylate (DMAEMA, 99%) were purchased from Aladdin Industrial Co. (China); MWCNTs was obtained from Beijing Dk Nano technology Co., Ltd. The ethanol, acetic acid, methanol, luminol and all the other chemicals unless specified were of analytical reagent grade and used without further purification.

TEOS and DMF were distilled under reduced vacuum pressure and DMAEMA was purified with alkaline Al_2O_3 column. Redistilled water was used throughout the work. Tris-HCl buffer (Tris buffer, pH = 7.4, 0.01 mol/L) solution was used in the experiment and were stored in refrigerator (4°C).

2.3 Apparatus

The IFFM-E flow injection CL analyser (Xi'an Remex Electronic instrument High-Tech Ltd., China) was equipped with an automatic injection system and a detection system. A certain amount of imprinting polymer (Fe_3O_4/MWCNTs/SiO_2-SMIP) and non-imprinting polymer (Fe_3O_4/MWCNTs/SiO_2-SNIP) were placed in front of the CL analyser as recognition elements. XRD measurement was made on a D8 focus spectrometer (Brooke AXS, Germany). The morphology of Fe_3O_4/MWCNTs/SiO_2 nanoparticles was characterized

5

121   with a Scanning Electron Microscope (SEM, GUANTA FEG 250, FEI, America).

122   **2.3 Preparation of dopamine coated Fe$_3$O$_4$ nanoparticles**

123   Dopamine coated Fe$_3$O$_4$ nanoparticles were synthesized according to a modified

124   procedure described in the previous literatures of our group and other people,

125   respectively [18, 26]. 0.15 g FeCl$_2$·4H$_2$O and 0.21 g FeCl$_3$·6H$_2$O were dissolved in

126   200 mL water with vigorous stirring under nitrogen protection. Then, 40 mL

127   NH$_3$·H$_2$O (28 wt %) solution was added into the solution dropwise. The system was

128   maintained at 80°C and the reaction was keeping for 30 min. Then, 5 mL acetic acid

129   (25%) solution was injected into the solution with sonication. The black precipitation

130   was separated with an external magnetic field, washed with water and ethanol

131   gradually to remove the unreacted chemicals, and then dried in vacuum drying

132   chamber at 60°C. Subsequently, 50 mg of dopamine hydrochloride was dissolved in

133   200 mL pH 4.0 acid solutions. 50 mg of as prepared Fe$_3$O$_4$ nanoparticles was then

134   added and stirred for 30 min. The obtained precipitate could be readily dispersed in

135   water and formed a stable colloid. The products (dopamine coated Fe$_3$O$_4$

136   nanoparticles) were collected by magnetic separation, washed with water and ethanol,

137   and then dried in the vacuum drying chamber at 50°C.

138   **2.4 Preparation of APTMS coated SiO$_2$ nanoparticles**

139   APTMS coated SiO$_2$ nanoparticles were prepared according to the previous

140   literatures [22, 27] with some modification. Briefly, 200 mL anhydrous ethanol and 12

141   mL NH$_3$·H$_2$O (25%-28%) was mixed under constant stirring for well-dispersion at

142   30°C. Then, 12 mL TEOS was added into the solution. The mixtures were reacted for

143   7 min at room temperature by constant mechanism stirring and the color of solution

144   was milky white. Subsequently, the reaction was continued overnight at 25°C by

145   stirring to form a homogeneous solution. The product of SiO$_2$ nanoparticles were

146   collected by centrifugation, and washed with water and ethanol, and then freeze-dried.

147   0.5 g as prepared SiO_2 nanoparticles was dispersed in 50 mL of anhydrous toluene.

148   Then, 5 mL of APTMS was added in the solution followed by refluxing at 80°C for

149   16 h. After centrifugation separated, washed by water and ethanol, dried in vacuum,

150   products (APTMS coated SiO_2 nanoparticles) were obtained.

151   **2.5 Preparation of Fe_3O_4/MWCNTs/SiO_2 nanoparticles**

152   The carboxylated MWCNTs (MWCNTs-COOH) were synthesized by refluxing

153   the MWCNTs in nitric acid solution (65-68 wt %) at 75°C for 11 h [28]. After cooling

154   to room temperature, the mixture was filtered and washed with double distilled water

155   until the pH values was 6.5 and finally dried at 60°C overnight. 0.3 g

156   MWCNTs-COOH was dispersed in 25 mL thionyl chloride solution by ultrasonication

157   (200W, 40 kHz). The mixture was further stirred vigorously and refluxed for 24 h at

158   50°C. Then the product (MWCNTs-COCl) was washed by anhydrous tetrahydrofuran

159   following dried at 50°C. 20 mg of MWCNTs-COCl, 10 mg dopamine coated Fe_3O_4

160   nanoparticles and 10 mg APTMS coated SiO_2 nanoparticles were scattered in 40 mL

161   DMF by ultrasonication which then was refluxed at 120°C for 24 h under the

162   protection of N_2. The obtained product (Fe_3O_4/MWCNTs/SiO_2) was then magnetically

163   separated, washed with water and ethanol and dried under vacuum.

164   **2.6 Preparation of Fe_3O_4/MWCNTs/SiO_2-SMIP and Fe_3O_4/MWCNTs/SiO_2-SNIP**

165   Fe_3O_4/MWCNTs/SiO_2-SMIP was synthesized according to a modified procedure

166   described in the previous literature [29]. The preparing process was shown in Fig. 1.

167   Solution A: MAA (0.1 mL), MA (32 mg) and DMAEMA (0.1 mL) were

168   dissolved in 30 mL Tris buffer solution and mixed thoroughly by ultrasonication.

169   Then, 32 mg of RNase A was dissolved to this solution by ultrasonication.

170   Solution B: 120 mg Fe_3O_4/MWCNTs/SiO_2 was dispersed in 15 mL ethanol and 5

7

171   mL Tris buffer solution which was then ultrasonicated to make it well-distributed.

172   Subsequently, freshly prepared solution B was added into solution A, and the mixture

173   was degassed for 10 min and purged with nitrogen stream for another 5 min. Then,

174   the solution was shaked for 1 h to preassemble. By adding 30 mg of APS, 0.4 mL

175   TEMED and 15 mg ferrous sulfate to the mixture, polymerization was initiated and

176   continued under violent starring at 25 ◦C for 10 min.

177   After the polymerization, the RNase A-imprinting particles were collected by

178   magnetic separation. The particles were washed with deionized water to remove

179   superfluous monomers. And then, they were washed repeatedly with 0.5 mol/L NaCl

180   solution to remove embedded template until no RNase A in the supernatant.

181   Subsequently, they were washed with Tris buffer solution to remove remained NaCl.

182   Finally, the Fe_3O_4/MWCNTs/SiO_2-SMIP was freeze-dried for further use. The

183   Fe_3O_4/MWCNTs/SiO_2-SNIP were prepared and washed in the same way but without

184   addition of RNase A.
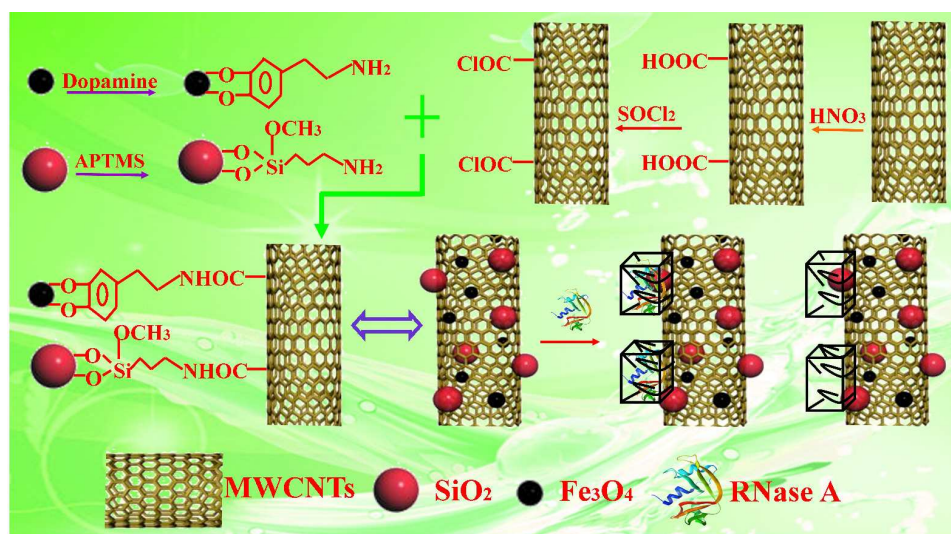
185

186   **Fig.1.** The preparing process of Fe_3O_4/MWCNTs/SiO_2-SMIP

187   **2.7 Binding performance of Fe₃O₄/MWCNTs/SiO₂-SMIP and Fe₃O₄/MWCNTs/**

188   **SiO₂-SNIP**

189   Batch adsorption experiments: 5.0 mg Fe_3O_4/MWCNTs/SiO_2-SMIP and Fe_3O_4/

190   MWCNTs/SiO_2-SNIP nanoparticles were placed into 5 mL centrifuge tubes,

191   respectively. Then, 2.0 mL of different concentration of RNase A solution was added

192   into the tube and the dispersion liquid was incubated at 25∘C for 1 h. After magnetic

193   separation, the concentration of the supernatant in the tube was determined by CL

194   instrument. Rebinding dynamics: 5.0 mg Fe_3O_4/MWCNTs/SiO_2-SMIP and

195   Fe_3O_4/MWCNTs/ SiO_2-SNIP nanoparticles were dispersed in 2.0 mL 2.0 mg/mL

196   RNase A solution which then were incubated at 25∘C for 1 min, 5 min, 10 min, 15

197   min, 20 min, 25 min and 30 min respectively. After magnetic separation, the

198   concentration of the supernatant in the tube was determined by CL instrument.

199   The amount of protein adsorbed by the particles was calculated from the

200   following formula.

$$Q = (c_0 - c_e)\frac{V}{m}$$

201

202   Where Q (mg/g) was the mass of protein adsorbed by unit mass of dry particles,

203   c_0 (mg/mL) and c_e (mg/mL) were the concentrations of RNase A in the initial and

204   final solutions, respectively, V (mL) was the volume of the adsorption mixture, and m

205   (g) was the mass of the Fe_3O_4/MWCNTs/SiO_2-SMIP (Fe_3O_4/MWCNTs/SiO_2-SNIP).

206   **3 Results and discussion**

207   **3.1 Characterization of Fe₃O₄/MWCNTs/SiO₂-SMIP**

208   The surface morphology of Fe_3O_4, MWCNTs, SiO_2 and Fe_3O_4/MWCNTs/SiO_2

209   was characterized by SEM and the results were shown in Fig. 2, respectively. From

210   Fig. 2 (A-B), dopamine coated Fe_3O_4 and SiO_2 nanoparticles were obtained with a

211 spherical morphology respectively. In Fig. 2 (D), Fe_3O_4/MWCNTs/SiO_2

212 nanocomposites showed that a network of MWCNTs was interwoven among the

213 Fe_3O_4 and SiO_2 particles and configuration was readily observed different from

214 MWCNTs greatly shown in Fig. 2 (C). With Fe_3O_4 and SiO_2 nanoparticles grown

215 along the MWCNTs, the imprinting sites situated at or near the surface of the material

216 could contribute to the mass transfer.
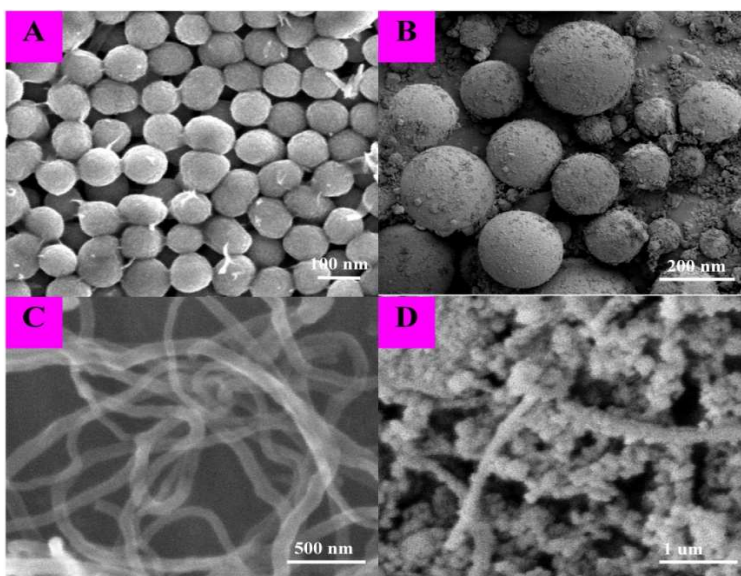
217

218 **Fig.2.** The SEM images of dopamine coated Fe_3O_4 (A), SiO_2 nanoparticles (B), MWCNTs (C) and

219 Fe_3O_4/MWCNTs/SiO_2 nanocomposite (D)

220 Fig. 3 (A) showed the XRD patterns of Fe_3O_4, MWCNTs, SiO_2 and Fe_3O_4/

221 MWCNTs/SiO_2 nanomaterials. The peaks at $2\theta = 30.3°$, $35.5°$, $43.2°$, $53.5°$, $57.4°$ and

222 $62.9°$ corresponding to (220), (311), (400), (422), (511) and (440) planes, respectively,

223 which can be indexed to be the six characteristic peaks of Fe_3O_4, were clearly

224 observed in the patterns of Fe_3O_4/MWCNTs/SiO_2. The broad and strong diffraction

225 peak in the pattern of Fe_3O_4/MWCNTs/SiO_2 around $2\theta = 23°$ overlapped the

226 characteristic peaks of SiO_2 ($2\theta = 22.5°$) [30] and MWCNTs ($2\theta = 25.5°$) [31], which

227 verified the successful formation of Fe_3O_4/MWCNTs/SiO_2 sufficiently.

228 Fig. 3 (B) showed the FTIR spectra of MWCNTs-COOH, dopamine coated

229   Fe_3O_4 nanoparticles, APTMS coated SiO_2 and Fe_3O_4/MWCNTs/SiO_2. The stretching

230   vibration of benzene ring contributed to the peaks between 1400-1600 cm^{-1} in the

231   figure. In the spectrum of dopamine coated Fe_3O_4, the peak at 630 cm^{-1} was due to

232   the interactions of Fe-O-Fe and 1200 cm^{-1} correspond to C-O stretching and

233   arylamine C-N stretching vibration together, which directly evidenced the preparation

234   of the dopamine coated Fe_3O_4. The two weak peaks in the spectrum of

235   MWCNTs-COOH at 1114 and 3011 cm^{-1} were for the stretching of C-O and C-H of

236   alkene respectively. The clearly observed broad and strong absorption peak around

237   1085 cm^{-1} was for the C-Si variable angle vibration and Si-O stretching vibration and

238   the peak at 1396 cm^{-1} corresponded to the C-H flexural mode. In addition, the weak

239   peak at 789 cm^{-1} was attributed to the Si-CH_2 stretching vibration. It was confirmed

240   the successful preparation of APTMS coated SiO_2. In the spectrum of

241   Fe_3O_4/MWCNTs/SiO_2, the existence of the peaks clearly observed overlapped the

242   corresponding peaks of MWCNTs-COOH, dopamine coated Fe_3O_4 and APTMS

243   coated SiO_2 which suggested the formation of the new material

244   Fe_3O_4/MWCNTs/SiO_2.
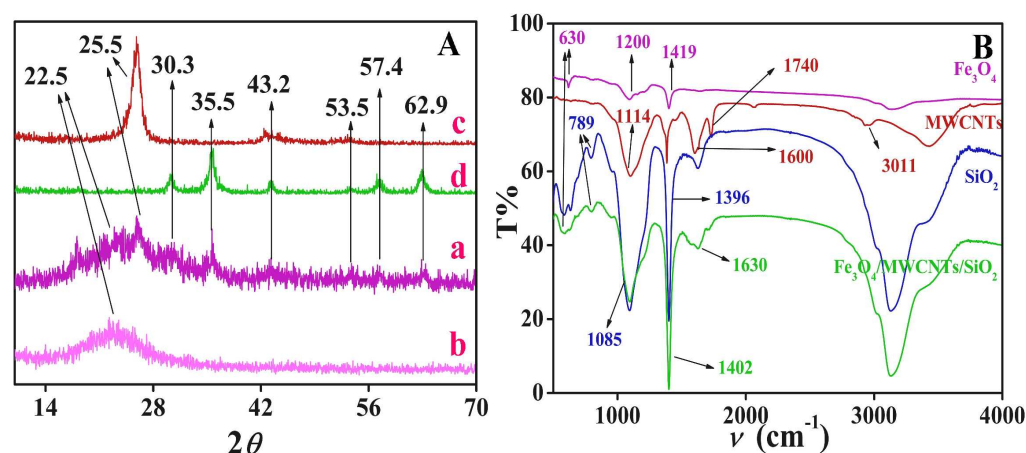
245

246   **Fig.3.** The XRD pattern (A) of Fe_3O_4/MWCNTs/SiO_2 (a), SiO_2 (b), MWCNTs (c) and Fe_3O_4 (d);

247   the FTIR spectra (B) of MWCNTs-COOH, dopamine coated Fe_3O_4, APTMS coated SiO_2 and

248   Fe_3O_4/MWCNTs/SiO_2 nanocomposite

11

249   **3.2 Binding performance of Fe$_3$O$_4$/MWCNTs/SiO$_2$-SMIP and Fe$_3$O$_4$/MWCNTs/**

250   **SiO$_2$-SNIP**

251   The adsorption performance of Fe$_3$O$_4$/MWCNTs/SiO$_2$-SMIP and Fe$_3$O$_4$/

252   MWCNTs/SiO$_2$-SNIP to RNase A was researched shown in Fig. 4. Adsorption

253   isotherms, i.e. binding capacities to RNase A at different initial concentrations, were

254   showed in Fig. 4 (A). The adsorption capacity to RNase A reached maximum 102

255   mg/g and was higher than that of the SNIP prepared at the same conditions. And in

256   order to compare, Fe$_3$O$_4$/MWCNTs-SMIP was prepared and the maximum adsorbing

257   capacity of Fe$_3$O$_4$/MWCNTs-SMIP was only 83.2 mg/g which demonstrated that SiO$_2$

258   played an important role in the preparation of proposed SMIP.

259   It was believed that the fabrication of Fe$_3$O$_4$/MWCNTs/SiO$_2$ nanocomposites

260   could not only maintain the adsorption behavior but also allow the compound to be

261   easily separated and recycled in practical applications. Theory adsorption capacity of

262   Fe$_3$O$_4$/MWCNTs/SiO$_2$-SMIP was described by Langmuir and Freundlich equations,

263   respectively. The Langmuir and Freundlich equations which were expressed in

264   following equation were used for modeling adsorption isotherms.

265     $$\text{Langmuir equations: } \frac{c_e}{q_e} = \frac{c_e}{q_m} + \frac{1}{q_m k_L} \qquad \text{Freundlich equation: } \ln q_e = \ln k_F + \frac{\ln c_e}{n}$$

266   Where c_e (mg/mL) is the equilibrium concentration of RNase A, q_e (mg/g) is the

267   adsorption capacity, q_m (mg/g) is the theoretical saturation adsorption capacity, k_L is

268   the Langmuir constant, k_F is the binding energy constant and n is the Freundlich

269   constant.

270   The linear fitting curves of the Langmuir and Freundlich models were shown in

271   Fig.5 (A, B) respectively. As we could see, the relative standard deviation values

272   indicated that the Langmuir isotherm were more appropriate than the Freundlich

273   model at the present temperature. Therefore, the adsorption of RNase A by

274   Fe_3O_4/MWCNTs/SiO_2-SMIP was monolayer uniform adsorption. Theory adsorption

275   capacity of Fe_3O_4/ MWCNTs/SiO_2-SMIP was obtained to be 106 mg/g which was

276   approximate to the experimental result 102 mg/g. The adsorption kinetics of

277   Fe_3O_4/MWCNTs/ SiO_2-SMIP and Fe_3O_4/MWCNTs/SiO_2-SNIP to RNase A were then

278   explored and shown in Fig. 4 (B). Because of the imprinting sites situated at or in the

279   proximity of the material's surface which could help mass transfer, adsorption

280   equilibrium could be achieved within 20 min contact time.

281
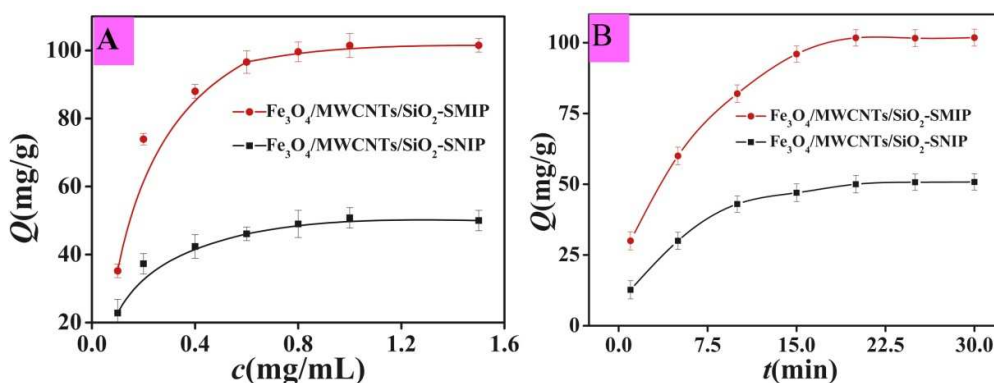
**Fig.4.** Adsorption isotherm curves (A) and kinetics curves (B) of Fe_3O_4/MWCNTs/SiO_2-SMIP

283   and Fe_3O_4/MWCNTs/SiO_2-SNIP
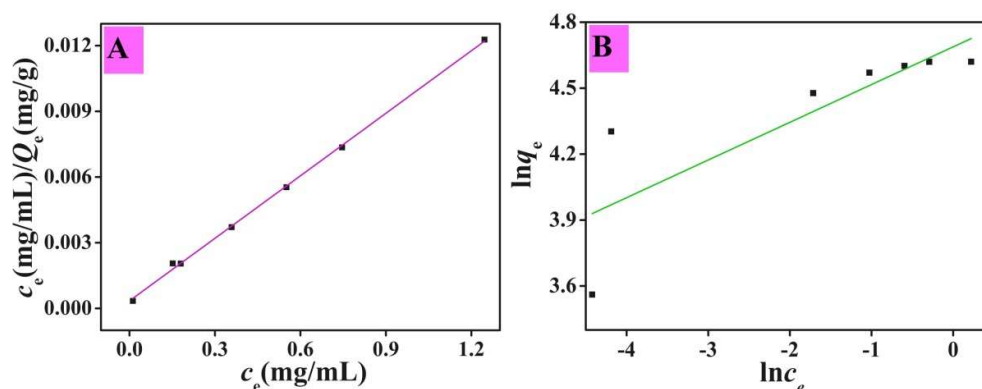
284

285   **Fig.5.** The Langmuir (A) and Freundlich (B) adsorption isotherm fit of RNase A

286   **3.3 Optimization of Fe_3O_4/MWCNTs/SiO_2-SMIP-CL sensor**

287   The optimization experiments were carried out to get a better knowledge of the

288   CL reaction of luminol-H_2O_2-RNase A. Peristaltic pumps speed was an important 鄂

289   effect factor in the experiments. When pump speed reached the best: 30r/min, the

290   effects of concentration of H_2O_2, NaOH and luminol on the CL intensity were

291   researched and the results were shown in Fig. 6 (A-C). Simultaneously, the optimal

292   concentration conditions were 0.05 mol/L of H_2O_2 solution, 0.003 mol/L of NaOH

293   solution and 5.0×10^{-3} mol/ L of luminol solution which were used throughout the

294   entire study.
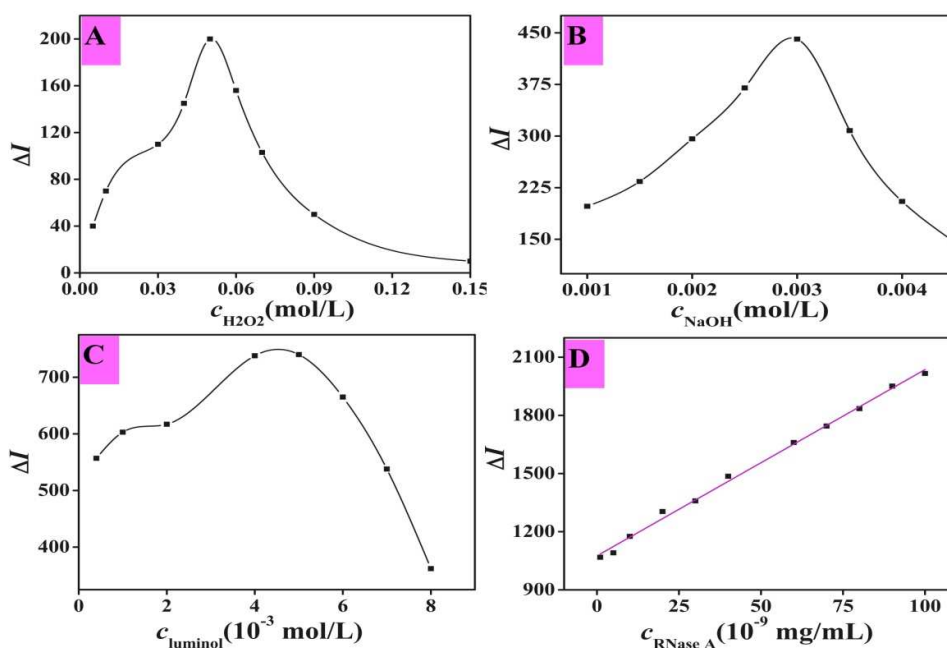
295

296   **Fig.6.** Optimization results: (A) Effect of H_2O_2 concentration on CL intensity. Conditions:

297   c(NaOH) = 0.1 mol/L, c(luminol) = 1.0×10^{-4} mol/L; (B) Effect of NaOH concentration on CL

298   intensity. Conditions: c(luminol) = 1.0×10^{-4} mol/L, c(H_2O_2) = 0.05 mol/L; (C) Effect of luminol

299   concentration on CL intensity. Conditions: c(H_2O_2) = 0.05 mol/L, c(NaOH) = 0.003 mol/L; (D)

300   The regression equation of the Fe_3O_4/MWCNTs/SiO_2-SMIP-CL sensor

301   **3.4 Analytical performance of Fe_3O_4/MWCNTs/SiO_2-SMIP-CL sensor**

302   The CL intensity responded linearly to the concentration of RNase A in the range

303   1.0×10^{-9} - 1.0×10^{-7} mg/mL with detection limit of 3.2×10^{-10} mg/mL (3δ) which

304   was superior to conventional methods shown in Table 1. The regression equation

305   was $\Delta I = 1069 + 9.6 \times 10^9$ c (mg/mL) with a correlation coefficient of 0.9961 as

306   shown in Fig. 6 (D). The relative standard deviation (RSD) for the determination of

307   1.0×10^{-8} mg/mL RNase A was 4.9% ($n = 11$). The results showed that

308   Fe$_3$O$_4$/MWCNTs/SiO$_2$-SMIP-CL sensor exhibited lower detection limit, high

309   accuracy, sensitivity and selectivity to RNase A conceivably.

310   **Table 1.** Comparing results with conventional methods

Method	Linear range (mg/mL)	Detection limit (mg/mL)
Our work	1.0×10^{-9} - 1.0×10^{-7}	3.2×10^{-10}
Gold electrode [5]	1.0×10^{-8} - 1.0×10^{-3}	1.0×10^{-8}
FRET-based probe [32]		1.0×10^{-6}
Electrochemical assay [33]	2.0×10^{-7} - 1.0×10^{-5}	2.0×10^{-7}

311   **3.5 Interferences studies**

312   The effects of foreign substances were examined by adding analytes with

313   increasing amounts in the standard solution of RNase A. The interferences study of

314   the imprinting nanoparticles was carried out with other three kinds of proteins: bovine

315   serum albumin (BSA), lysozyme (Lys) and bovine hemoglobin (BHb). The tolerable

316   limit of coexisted species was less than ±5%. The detail was shown in Table 2. In the

317   CL system, 250 times Na$^+$ and K$^+$ concentration (compared with RNase A)

318   interfered with the determination of RNase A but when using

319   Fe$_3$O$_4$/MWCNTs/SiO$_2$-SMIP-CL, 800 times Na$^+$ and K$^+$ concentration would interfere

320   with the determination of RNase A for the imprinting cavities which were suitable for

321   macromolecule and could recognize and absorb RNase A specifically. Then, the

322   interferences from L-phenylalanine and Chrysoidine were slightly less. On the

323   contrary, the interferences from BSA, Lys and BHb were more serious relatively. But

324   from Table 2, it was convinced to say that the application of

325   Fe$_3$O$_4$/MWCNTs/SiO$_2$-SMIP in CL sensor could eliminate or reduce the interference

326 directly.

327 **Table 2.** The tolerable ratio of interfering species to RNase A

Species	Na^+, K^+	L-phenylalanine	Chrysoidine	Lys	BHb	BSA
Fe_3O_4/MWCNTs/SiO_2-SMIP-CL	900	700	600	150	80	60
CL	250	210	150	65	45	25

328 **3.6. Reusability of Fe_3O_4/MWCNTs/SiO_2-SMIP**

329 The reusability of Fe_3O_4/MWCNTs/SiO_2-SMIP was an important parameter of

330 the sensor. The RNase A absorbed in Fe_3O_4/MWCNTs/SiO_2-SMIP was extracted with

331 0.5 mol/L NaCl and water respectively for several times until no RNase A in the

332 supernatant. It could be acquired that there was only 13% binding capacity loss within

333 7 times of Fe_3O_4/MWCNTs/SiO_2-SMIP to the concentration of 1.0×10^{-8} mg/mL

334 RNase A, which powerfully certified that Fe_3O_4/MWCNTs/SiO_2-SMIP performed

335 excellently reusability in the detection of RNase A in practical samples.

336 **3.7 Practical sample analysis and the application of the sensor**

337 **Table 3.** Practical sample analysis and the application of the sensor

Sample	c /(10^{-8} mg/mL) (n=6)	RSD%	Added (10^{-8} mg/mL)	Found (10^{-8} mg/mL) (n=6)	Recovery%
1[#]	2.1	3.2	5.0	6.8	94
2[#]	4.7	3.3	5.0	9.7	100
3[#]	5.5	3.7	5.0	10.8	105
4[#]	8.7	3.5	5.0	13.1	93

338 As shown in Table 3, Fe_3O_4/MWCNTs/SiO_2-SMIP-CL sensor was applied in

339 biological samples under optimal experimental conditions. To validate this proposed

340 sensor, recoveries were obtained ranging from 93% to 105%. Obviously, these results

341 showed that the sensor had good accuracy. Hence, it was entirely feasible that the

16

342   Fe_3O_4/MWCNTs/SiO_2-SMIP-CL sensor could be used in the detection of RNase A in

343   practical samples.

4 Conclusion

345   In this work, with a new material of Fe_3O_4/MWCNTs/SiO_2 used as supporting

346   material in the preparation of SMIP, a CL sensor for highly sensitive determination of

347   RNase A was proposed. Compared with core-shell $Fe_3O_4@SiO_2$/MWCNTs

348   nanocomposite, Fe_3O_4 could not only serve as backbone material in the preparation of

349   RNase A SMIP, but also as separation reagent to make the collection of SMIP

350   complex easily, carbon nanotube and SiO_2 was used as supporting material to bear

351   SMIP for their large specific surface area. The adsorption ability of the

352   Fe_3O_4/MWCNTs/SiO_2-SMIP was evaluated to be 102 mg/g and the Langmuir

353   isotherm was more appropriate than the Freundlich model at the present temperature.

354   Finally, the CL sensor based on Fe_3O_4/MWCNTs/SiO_2-SMIP was prepared for

355   determination of RNase A. Application of new material Fe_3O_4/MWCNTs/SiO_2 to the

356   sensor in literature at the moment is very meritorious in determination of RNase A for

357   high accuracy, selectivity and sensitivity.

Acknowledgements

363

Reference

[1] V. Parmenopoulou, D.S.M. Chatzileontiadou, S. Manta, S. Bougiatioti, P. Maragozidis, D.N. Gkaragkouni, et al., Triazole pyrimidine nucleosides as inhibitors of Ribonuclease A. Synthesis, biochemical, and structural evaluation. Bioorg Med Chem 2012, 20(24): 7184-7193.

[2] R.T. Rains, Ribonuclease A. Chem Rev 1998, 98(3): 1045-1066.

[3] L. Ledoux, Action of ribonuclease on two solid tumors *in vivo*. Nature 1955, 176(4470): 36-37.

[4] J.H. Choi, J.Y. Jang, Y.K. Joung, M.H. Kwon, K.D. Park, Intracellular delivery and anti-cancer effect of self-assembled heparin-Pluronic nanogels with RNase A. J Control Release 2010, 147(3): 420-427.

[5] W.C. Kim, C.H. Lee, The role of mammalian ribonucleases (RNases) in cancer. Biochim Biophys Acta 2009, 1796(2): 99-113.

[6] S. Sato, S. Takenaka, Electrochemical RNase A detection using an electrode with immobilized ferrocenyl deoxyribooligonucleotide containing cytidine residue. Electroanalysis 2013, 25(7): 1652-1658.

[7] F.H. Dickey, The preparation of specific adsorbents. Proc Natl Acad Sci U S A. 1949, 35(5): 227-229.

[8] G. Wulff, A. Sarhan, K. Zabrocki, Enzyme-analogue built polymers and their use for the resolution of racemates, Tetrahedron Lett 1973, 14(44): 4329-4332.

[9] B. Sellergren, Polymer- and template-related factors influencing the efficiency in olecularly imprinted solid-phase extractions. TrAC 351 Trends Anal Chem 1999,

386   18(3): 164-74.

387   [10] P. Curcio, C. Zandanel, A. Wagner, C. Mioskowski, R. Baati, Semi-covalent

388   surface molecular imprinting of polymers by one-stage mini-emulsion

389   polymerization: glucopyranoside as a model analyte. Macromol Biosci 2009,

390   9(6): 596-604.

391   [11] C.S. Mahon, D.A. Fulton, Mimicking nature with synthetic macromolecules

392   capable of recognition. Nature Chem 2014, 6: 665-672.

393   [12] H.Q. Shi, W.B. Tsai, M.D. Garrison, S. Ferrari, B.D. Ratner, Template-imprinted

394   nanostructured surfaces for protein recognition. Nature 1999, 398: 593-597.

395   [13] T. Chen, M. Shao, H. Xu, S. Zhuo, S. Liu, S.T. Lee, Molecularly imprinted

396   polymer-coated silicon nanowires for protein specific recognition and fast

397   separation. J Mater Chem 2012, 22: 3990-3996.

398   [14] H. Zhang, Q. Liu, J. Wang, J. Liu, H. Yan, X. Jing, B. Zhang, Preparation of

399   magnetic calcium silicate hydrate for the efficient removal of uranium from

400   aqueous systems. RSC Adv 2015, 5: 5904-5912.

401   [15] J. Yang, H. Xiang, L. Shuai, S. Gunasekaran. A sensitive enzymeless hydrogen-

402   peroxide sensor based on epitaxially-grown Fe_3O_4 thin film. Anal Chim Acta

403   2011, 708(1-2): 44-51.

404   [16] L. Wang, S. Hong, L. Wang, L. Dong, G. Bian, H. Chen, Novel magnetic and

405   fluorescent nanocomposite as a sensitive probe for the determination of proteins.

406   Spectrochimica Acta A 2006, 65(2): 439-444.

407   [17] Q.Q. Gai, F. Qu, Z.J. Liu, R.J. Dai, Y.K. Zhang, Superparamagnetic lysozyme

408   surface-imprinted polymer prepared by atom transfer radical polymerization and

409   its application for protein separation. J Chromatogra A 2010, 1217: 5035-5042.

410   [18] A. Walter, C. Billotey, A. Garofalo, U Corinne, J. Taleb, Mastering the shape and

411   composition of dendronized iron oxide nanoparticles to tailor magnetic

412   resonance imaging and hyperthermia. Chem Mater 2014, 26(18): 5252-5264.

413   [19] C. Chao, J. Liu, J. Wang, Y. Zhang, B. Zhang, Y. Zhang, et al., Surface

414   Modification of Halloysite Nanotubes with Dopamine for Enzyme

415   Immobilization. ACS Appl Mater Interfaces 2013, 5(21): 10559-10564.

416   [20] W. Jin, L. Yang, W. Yang, B. Chen, Grafting of HEMA onto dopamine coated

417   stainless steel by 60Co-γ irradiation method. Radia Phys Chem 2014, 105: 57-62

418   [21] Z. Liu, L. Ji, X. Dong, Z. Li, L. Fu, Q. Wang, Preparation of Co-N-C supported

419   on silica spheres with high catalytic performance for ethylbenzene oxidation.

420   RSC Adv 2015, 5: 6259-6264.

421   [22] G. Fu, H. He, Z. Chai, H. Chen, J. Kong, Y. Wang, et al., Enhanced lysozyme

422   imprinting over nanoparticles functionalized with carboxyl groups for

423   noncovalent template sorption. Anal Chem 2011, 83: 1431-1436.

424   [23] M.S. Zhang, J.R. Huang, P. Yu, X. Chen, Preparation and characteristics of

425   protein molecularly imprinted membranes on the surface of multiwalled carbon

426   nanotubes. Talanta 2010, 81: 162-166.

427   [24] Y. Peng, Z. Wu, Z. Liu, An electrochemical sensor for paracetamol based on an

428   electropolymerized molecularly imprinted o-phenylenediamine film on a

429   multi-walled carbon nanotube modified glassy carbon electrode. Anal Method

430   2014, 6: 5673-5681.

431   [25] M. Arvand, M. Hassannezhad, Magnetic core-shell $Fe_3O_4@SiO_2$/MWCNT

432   nanocomposite modified carbon paste electrode for amplified electrochemical

433   sensing of uric acid. Mater Sci Eng C 2013, 36: 160-167.

434   [26] P. An, F. Zuo, Y.P. Wue, J.H. Zhang, Z.H.Zheng, X.B.Ding, et al., Fast synthesis

435   of dopamine-coated Fe_3O_4 nanoparticles through ligand-exchange method.

436   Chinese Chem Lett 2012, 23: 1099-1102.

437   [27] D. Li, D. Wan, X. Zhu, Y. Wang, S. Han, Broadband antireflection TiO_2-SiO_2

438   stack coatings with refractive-index-grade structure and their applications to

439   Cu(In, Ga)Se_2 solar cells. Sol Energy Mat Sol Cells 2014, 130: 505-512.

440   [28] H.J. Chen, Z.H. Zhang, L.J. Luo, S.Z. Yao, Surface-imprinted chitosan-coated

441   magnetic nanoparticles modified multi-walled carbon nanotubes biosensor for

442   detection of bovine serum albumin. Sensor Actuat B 2012, 163: 76-83.

443   [29] H.Y. He, G.Q. Fu, Y. Wang, Z.H. Chai, Y.Z. Jiang, Z.L. Chen, Imprinting of

444   protein over silica nanoparticles via surface graft copolymerization using low

445   monomer concentration. Biosens Bioelectron 2010, 26: 760-765.

446   [30] H. Liu, Z. Jia, S. Ji, Y. Zheng, M. Li, H. Yang, Synthesis of TiO_2/$SiO_2@Fe_3O_4$

447   magnetic microspheres and their properties of photocatalytic degradation

448   dyestuff. Catal Today 2011, 175: 293-298.

449   [31] L. Zhi, Q. Zhang, T. Wei, J. Feng, M. Zhang, W. Qian, A three-dimensional

450   carbon nanotube/graphene sandwich and its application as electrode in

451   supercapacitors Adv Mater 2010, 22: 3723-3728.

452   [32] B. Kelemen, T. Klink, M. Behlke, S. Eubanks, R. Raines, Hypersensitive

453   substrate for ribonucleases. Nucleic Acids Res 1999, 27(18): 3696-3701.

454   [33] M. Kanazawa, S. Sato, S. Takenaka, Ferrocenylnaphthalene diimide-based

455   electrochemical ribonuclease assays. Anal Sci 2007, 23(12), 1415-1419.